

# Constraints on the CMB Temperature Evolution using Multi-Band Measurements of the Sunyaev Zel'dovich Effect with the South Pole Telescope

A. Saro<sup>1,2</sup>, J. Liu<sup>1,2</sup>, J. J. Mohr<sup>1,2,3</sup>, K. A. Aird<sup>4</sup>, M. L. N. Ashby<sup>5</sup>, M. Bayliss<sup>5,6</sup>,  
 B. A. Benson<sup>7,8,9</sup>, L. E. Bleem<sup>8,10,11</sup>, S. Bocquet<sup>1,2</sup>, M. Brodwin<sup>12</sup>,  
 J. E. Carlstrom<sup>8,9,10,11,13</sup>, C. L. Chang<sup>8,9,11</sup>, I. Chiu<sup>1,2</sup>, H. M. Cho<sup>14</sup>, A. Clocchiatti<sup>15</sup>,  
 T. M. Crawford<sup>8,13</sup>, A. T. Crites<sup>8,13</sup>, T. de Haan<sup>16</sup>, S. Desai<sup>1,2</sup>, J. P. Dietrich<sup>1,2</sup>,  
 M. A. Dobbs<sup>16</sup>, K. Dolag<sup>1,2</sup>, J. P. Dudley<sup>16</sup>, R. J. Foley<sup>17,18</sup>, D. Gangkofner<sup>1,2</sup>,  
 E. M. George<sup>19</sup>, M. D. Gladders<sup>8,13</sup>, A. H. Gonzalez<sup>20</sup>, N. W. Halverson<sup>21</sup>,  
 C. Hennig<sup>1,2</sup>, W. L. Holzapfel<sup>19</sup>, J. D. Hrubes<sup>4</sup>, C. Jones<sup>5</sup>, R. Keisler<sup>8,10</sup>, A. T. Lee<sup>19,22</sup>,  
 E. M. Leitch<sup>8,13</sup>, M. Lueker<sup>19,23</sup>, D. Luong-Van<sup>4</sup>, A. Mantz<sup>8</sup>, D. P. Marrone<sup>24</sup>,  
 M. McDonald<sup>25</sup>, J. J. McMahon<sup>26</sup>, J. Mehl<sup>8,13</sup>, S. S. Meyer<sup>8,9,10,13</sup>, L. Mocuano<sup>8,13</sup>,  
 T. E. Montroy<sup>27</sup>, S. S. Murray<sup>5</sup>, D. Nurgaliev<sup>6</sup>, S. Padin<sup>8,13,23</sup>, A. Patej<sup>6</sup>, C. Pryke<sup>28</sup>,  
 C. L. Reichardt<sup>19</sup>, A. Rest<sup>29</sup>, J. Ruel<sup>6</sup>, J. E. Ruhl<sup>27</sup>, B. R. Saliwanchik<sup>27</sup>, J. T. Sayre<sup>27</sup>,  
 K. K. Schaffer<sup>8,9,30</sup>, E. Shirokoff<sup>19,23</sup>, H. G. Spieler<sup>22</sup>, B. Stalder<sup>5</sup>, Z. Staniszewski<sup>27</sup>,  
 A. A. Stark<sup>5</sup>, K. Story<sup>8,10</sup>, A. van Engelen<sup>16</sup>, K. Vanderlinde<sup>31,32</sup>, J. D. Vieira<sup>17,23</sup>,  
 A. Vikhlinin<sup>5</sup>, R. Williamson<sup>8,13</sup>, O. Zahn<sup>19</sup>, A. Zenteno<sup>1,2</sup>

<sup>1</sup>Department of Physics, Ludwig-Maximilians-Universität, Scheinerstr. 1, 81679 München, Germany

<sup>2</sup>Excellence Cluster Universe, Boltzmannstr. 2, 85748 Garching, Germany

<sup>3</sup>Max-Planck-Institut für extraterrestrische Physik, Giessenbachstr. 85748 Garching, Germany

<sup>4</sup>University of Chicago, 5640 South Ellis Avenue, Chicago, IL 60637

<sup>5</sup>Harvard-Smithsonian Center for Astrophysics, 60 Garden Street, Cambridge, MA 02138

<sup>6</sup>Department of Physics, Harvard University, 17 Oxford Street, Cambridge, MA 02138

<sup>7</sup>Center for Particle Astrophysics, Fermi National Accelerator Laboratory, Batavia, IL, USA 60510

<sup>8</sup>Kavli Institute for Cosmological Physics, University of Chicago, 5640 South Ellis Avenue, Chicago, IL 60637

<sup>9</sup>Enrico Fermi Institute, University of Chicago, 5640 South Ellis Avenue, Chicago, IL 60637

<sup>10</sup>Department of Physics, University of Chicago, 5640 South Ellis Avenue, Chicago, IL 60637

<sup>11</sup>Argonne National Laboratory, 9700 S. Cass Avenue, Argonne, IL, USA 60439

<sup>12</sup>Department of Physics and Astronomy, University of Missouri, 5110 Rockhill Road, Kansas City, MO 64110

<sup>13</sup>Department of Astronomy and Astrophysics, University of Chicago, 5640 South Ellis Avenue, Chicago, IL 60637

<sup>14</sup>NIST Quantum Devices Group, 325 Broadway Mailcode 817.03, Boulder, CO, USA 80305

<sup>15</sup>Departamento de Astronomía y Astrofísica, Pontificia Universidad Católica, Chile

<sup>16</sup>Department of Physics, McGill University, 3600 Rue University, Montreal, Quebec H3A 2T8, Canada

<sup>17</sup>Astronomy Department, University of Illinois at Urbana-Champaign, 1002 W. Green Street, Urbana, IL 61801 USA

<sup>18</sup>Department of Physics, University of Illinois Urbana-Champaign, 1110 W. Green Street, Urbana, IL 61801 USA

<sup>19</sup>Department of Physics, University of California, Berkeley, CA 94720

<sup>20</sup>Department of Astronomy, University of Florida, Gainesville, FL 32611

<sup>21</sup>Department of Astrophysical and Planetary Sciences and Department of Physics, University of Colorado, Boulder, CO 80309

<sup>22</sup>Physics Division, Lawrence Berkeley National Laboratory, Berkeley, CA 94720

<sup>23</sup>California Institute of Technology, 1200 E. California Blvd., Pasadena, CA 91125

<sup>24</sup>Steward Observatory, University of Arizona, 933 North Cherry Avenue, Tucson, AZ 85721

<sup>25</sup>Kavli Institute for Astrophysics and Space Research, Massachusetts Institute of Technology, 77 Massachusetts Avenue, Cambridge, MA 02139

<sup>26</sup>Department of Physics, University of Michigan, 450 Church Street, Ann Arbor, MI, 48109

<sup>27</sup>Physics Department, Center for Education and Research in Cosmology and Astrophysics, Case Western Reserve University, Cleveland, OH 44106

<sup>28</sup>Physics Department, University of Minnesota, 116 Church Street S.E., Minneapolis, MN 55455

<sup>29</sup>Space Telescope Science Institute, 3700 San Martin Dr., Baltimore, MD 21218

<sup>30</sup>Liberal Arts Department, School of the Art Institute of Chicago, 112 S Michigan Ave, Chicago, IL 60603

<sup>31</sup>Dunlap Institute for Astronomy & Astrophysics, University of Toronto, 50 St George St, Toronto, ON, M5S 3H4, Canada

<sup>32</sup>Department of Astronomy & Astrophysics, University of Toronto, 50 St George St, Toronto, ON, M5S 3H4, Canada

**ABSTRACT**

The adiabatic evolution of the temperature of the cosmic microwave background (CMB) is a key prediction of standard cosmology. We study deviations from the expected adiabatic evolution of the CMB temperature of the form  $T(z) = T_0(1+z)^{1-\alpha}$  using measurements of the spectrum of the Sunyaev Zel’dovich Effect with the South Pole Telescope (SPT). We present a method for using the ratio of the Sunyaev Zel’dovich signal measured at 95 and 150 GHz in the SPT data to constrain the temperature of the CMB. We demonstrate that this approach provides unbiased results using mock observations of clusters from a new set of hydrodynamical simulations. We apply this method to a sample of 158 SPT-selected clusters, spanning the redshift range  $0.05 < z < 1.35$ , and measure  $\alpha = 0.017^{+0.030}_{-0.028}$ , consistent with the standard model prediction of  $\alpha = 0$ . In combination with other published results, we constrain  $\alpha = 0.011 \pm 0.016$ , an improvement of  $\sim 20\%$  over published constraints. This measurement also provides a strong constraint on the effective equation of state in models of decaying dark energy  $w_{\text{eff}} = -0.987^{+0.016}_{-0.017}$ .

**1 INTRODUCTION**

The existence of the cosmic microwave background is a fundamental prediction of the Hot Big Bang Theory. The intensity spectrum of the CMB radiation locally has been measured by the COBE FIRAS instrument and found to have a nearly exact blackbody spectrum with a temperature of  $T_0 = 2.72548 \pm 0.00057$  K (Fixsen et al. 2009).

A second fundamental prediction of the hot Big Bang theory is that the CMB temperature must evolve over cosmic time. Specifically, it is expected to evolve as  $T(z) = T_0(1+z)$ , under the assumption that the CMB photon fluid reacts adiabatically to the expansion of the Universe as described by general relativity and electromagnetism. Deviations from the adiabatic evolution of  $T(z)$  would imply either a violation of the hypothesis of local position invariance, and therefore of the equivalence principle, or that the number of photons is not conserved. In the former case, this could be associated with variations of dimensionless coupling constants like the fine-structure constant (see, e.g., Martins 2002, Murphy et al. 2003, Srianand et al. 2004). The latter case is a consequence of many physical processes predicted by non-standard cosmological models, such as decaying vacuum energy density models, coupling between photons and axion-like particles, and modified gravity scenarios. (e.g., Matyjasek 1995; Overduin & Cooperstock 1998; Lima et al. 2000; Puy 2004; Jaeckel & Ringwald 2010; Jetzer & Tortora 2011). In all of these models, energy has to be slowly injected or removed from the CMB without distorting the Planck Spectrum sufficiently to violate constraints from FIRAS (Avgoustidis et al. 2012).

Observational tests of non-standard temperature evolution typically are parametrized by very simple models for the deviation. In particular, we consider here the scaling law proposed by Lima et al. (2000):  $T(z) = T_0(1+z)^{1-\alpha}$ , with  $\alpha$  being a free constant parameter<sup>1</sup>. This is the phenomenological parametrization that has been most widely studied by previous authors; deviations of  $\alpha$  from zero would result as a consequence of one of the scenarios described above, such as the non-conservation of photon number.

To date, two different observables have been used to determine  $T(z)$ . At intermediate redshifts ( $z \lesssim 1.5$ ),  $T(z)$  can be determined from measurements of the spectrum of the Sunyaev-Zel’dovich effect (SZE) (Sunyaev & Zel’dovich 1972), a technique first suggested by Fabbri et al. (1978); Rephaeli (1980). The first attempt

to measure  $T(z)$  using the spectrum of the SZE was reported in Battistelli et al. (2002) using multi-frequency observations of the clusters A2163 and Coma. Luzzi et al. (2009) reported results from the analysis of a sample of 13 clusters with  $0.23 \leq z \leq 0.546$ . Adopting a flat prior on  $\alpha \in [0, 1]$ , they provided constraints  $\alpha = 0.024^{+0.068}_{-0.024}$ , consistent with standard adiabatic evolution.

At high redshift ( $z \gtrsim 1$ ), the CMB temperature can be determined from quasar absorption line spectra which show atomic or molecular fine structure levels excited by the photo-absorption of the CMB radiation. If the system is in thermal equilibrium with the CMB, then the excitation temperature of the energy states gives the temperature of the black-body radiation (e.g., Srianand et al. 2000; Molaro et al. 2002; Srianand et al. 2008). For example, Noterdaeme et al. (2011) have reported on a sample of five carbon monoxide absorption systems up to  $z \sim 3$  where the CMB temperature has been measured. They used their sample, in combination with low redshift SZE measurements to place constraints on the phenomenological parameter  $\alpha = -0.007 \pm 0.027$ . This also allowed them to put strong constraints on the effective equation of state of decaying dark energy models  $w_{\text{eff}} = -0.996 \pm 0.025$ . Recently, Avgoustidis et al. (2012) extended this analysis by including constraints inferred from differences between the angular diameter and luminosity distances (the so-called distance-duality relation), which is also affected in models in which photons can be created or destroyed. They also showed that by releasing the positive prior assumption on  $\alpha$  the same cluster sample studied in Luzzi et al. (2009) constrains  $\alpha = 0.065 \pm 0.080$ .

More recently, Muller et al. (2013) fit molecular absorption lines towards quasars to measure the CMB temperature with an accuracy of a few percent at  $z = 0.89$ . Combining their data with the data presented in Noterdaeme et al. (2011) they were able to further constrain  $\alpha = 0.009 \pm 0.019$ .

Constraints on the CMB redshift evolution can be significantly improved by including measurements of the SZE spectrum from experiments, such as the South Pole Telescope (SPT) and Planck, with much larger cluster samples. For instance, de Martino et al. (2012) forecast the constraining power of Planck (further discussed in 5) to measure  $\alpha$ . Using only clusters at  $z < 0.3$ , they predicted that Planck could measure  $\alpha$  with an accuracy  $\sigma_\alpha = 0.011$ .

In this work, we present constraints on the temperature evolution of the CMB using SZE spectral measurements at the 95 and 150 GHz bands from the South Pole Telescope. The SPT is a 10m millimetre-wave telescope operating at the South Pole (Carlstrom et al. 2011) that has recently completed a 2500 deg<sup>2</sup> multi-frequency survey of the southern extragalactic sky. Here we focus on the SZE selected cluster sample that lies within a 720 deg<sup>2</sup>

<sup>1</sup> In previous literature this parameter has been referred to with the Greek letter  $\alpha$  or  $\beta$ . To avoid confusion with the variable  $\beta = v/c$  defined in Eq. 1, we use  $\alpha$ .

subregion where optical follow-up and redshift measurements are complete (Song et al. 2012; Reichardt et al. 2013).

## 2 METHOD

Inverse Compton scattering of the CMB photons by the hot intra-cluster medium induces secondary CMB temperature anisotropies in the direction of clusters of galaxies. Neglecting relativistic corrections, the thermal (tSZE) and kinematic (kSZE) contribution to the temperature anisotropy in the direction  $\hat{n}$  of a cluster at a frequency  $\nu$  can be approximated by (de Martino et al. 2012):

$$\Delta T(\hat{n}, \nu) \simeq T_0(\hat{n})[G(\nu)y_c(\hat{n}) - \tau\beta]. \quad (1)$$

Here  $T_0(\hat{n})$  is the current CMB temperature at the direction  $\hat{n}$ ,  $\beta$  is the line of sight velocity of the cluster in the CMB frame in units of the speed of light  $c$  and  $\tau$  is the optical depth. The Comptonization parameter  $y_c$  is related to the integrated pressure along the line of sight  $y_c = (k_B\sigma_T/m_e c^2) \int n_e T_e dl$  (where  $n_e$  and  $T_e$  are respectively the electron density and temperature). In the non-relativistic regime and for adiabatic expansion,  $G(x) = x \coth(x/2) - 4$ , where the reduced frequency  $x$  is given by  $x = h\nu(z)/k_B T(z) = h\nu_0(1+z)/[k_B T_0(1+z)] \equiv x_0$  and is independent of redshift,  $\nu(z)$  is the frequency of a CMB photon scattered by the intra-cluster medium and  $T(z)$  is the black body temperature of the CMB at the cluster location.

If  $T(z) = T_0(1+z)^{1-\alpha}$ , then the reduced frequency varies as  $x(z, \alpha) = x_0(1+z)^\alpha$  and the spectral frequency dependence of  $G(\nu)$ , the tSZE, now also depends on  $\alpha$ :  $G(x) = G(\nu_0, \alpha, z)$ . From Eq. 1, neglecting the kSZE contribution, it follows that measuring the ratio of temperature decrements at two different frequencies  $\nu_1$  and  $\nu_2$  provides:

$$R(\nu_1, \nu_2, z, \alpha) \equiv \frac{\Delta T(\hat{n}, \nu_1, z)}{\Delta T(\hat{n}, \nu_2, z)} \simeq \frac{G(\nu_1, z, \alpha)}{G(\nu_2, z, \alpha)} \quad (2)$$

This ratio is redshift independent for  $\alpha = 0$ , but not in the case of  $\alpha \neq 0$ . This method has the advantage that, by taking ratios, the dependence on the Comptonization parameter  $y_c$  (and therefore on the cluster properties) is removed and the need to account for model uncertainties on the gas density and temperature profile is avoided (Battistelli et al 2002, Luzzi et al 2009). Note that in this approach the distribution of temperature ratios is, in general, non-Gaussian (Luzzi et al. 2009) and needs to be properly modelled.

One important source of noise in these measurements is the primary anisotropy of the CMB. To precisely measure  $\Delta T(\hat{n}, \nu)$  for a single cluster, we would have to remove the primary CMB anisotropies in the direction  $\hat{n}$ . In principle, this could be done by subtracting the CMB temperature measured near the SZE null frequency, which, in the case of  $\alpha = 0$  and non-relativistic ICM, is given by a map obtained at 217 GHz (de Martino et al. 2012). Alternatively, because the primary CMB fluctuations are random, it is possible reduce this source of noise by averaging over a large sample of clusters.

In Reichardt et al. (2013), the SPT cluster sample was selected using a matched multi-frequency spatial filter (Melin et al. 2006), designed to optimally measure the cluster signal given knowledge of the cluster profile and the noise in the maps. The cluster gas profiles are assumed to be well fit by a spherical  $\beta$  model (Cavaliere & Fusco-Femiano 1976), with  $\beta = 1$  and twelve possible core radii,  $\theta_c$ , linearly spaced from 0.25 to 3 arcmin. The noise contributions include astrophysical (e.g., the CMB, point sources) and instrumental (e.g., atmospheric, detector) contributions. For

each cluster, the maximum signal to noise in the spatially filtered maps was denoted as  $\xi$ .

In this work, we measure the ratio of the CMB temperature decrements in the SPT data at 95 and 150 GHz. We extract the cluster signal from the single-frequency spatially filtered maps at 95 and 150 GHz, using the SPT position and core radius favored by the multi-frequency analysis in Reichardt et al. (2013). To compare the decrement at each frequency, we need to account for the smaller beam at 150 GHz. We do this by convolving the 150 GHz data to the same beam size as the 95 GHz data, and then using the 95 GHz filter to extract the signal from the resultant 150 GHz maps. The associated uncertainty in the CMB temperature decrement would be equal to the R.M.S. of the single-frequency spatially filtered maps.

Finally, we use the derived values of temperature in the two bands and the associated cluster redshift to constrain  $\alpha$  from Eq. 2 through a maximum likelihood analysis (Luzzi et al. 2009) where the likelihood is defined as :

$$\mathcal{L}(\alpha) \propto \prod_{i=1}^{N_{\text{clus}}} \exp \left\{ -\frac{(T_{150}^{(i)} R(z^{(i)}, \alpha) - T_{95}^{(i)})^2}{2[(\Delta T_{150}^{(i)} R(z^{(i)}, \alpha))^2 + (\Delta T_{95}^{(i)})^2]} \right\}, \quad (3)$$

and  $R(z, \alpha) \equiv R(95 \text{ GHz}, 150 \text{ GHz}, z, \alpha)$  according to Eq. 2 is calculated by integrating:

$$R(z, \alpha) = \frac{\int G(\nu, z, \alpha) F_{95}(\nu) d\nu}{\int G(\nu, z, \alpha) F_{150}(\nu) d\nu}, \quad (4)$$

where  $F_{95}$  and  $F_{150}$  are the measured filter response of the SPT 95 and 150 GHz bands, normalized such that the integral over each of the bands is one. We have assumed the non-relativistic expression for  $G(\nu, z, \alpha)$ , however, we find relativistic corrections have a negligible effect on our result. For the range of electron temperatures expected in our cluster sample, including relativistic corrections from Itoh et al. (1998) changes our final constraints on  $\alpha$  by less than 1 per cent.

## 3 VERIFICATION OF METHOD WITH SIMULATIONS

We test the method described above using simulations. To do so, we make mock SPT observations of clusters that are formed in a large volume, high resolution cosmological hydrodynamical simulation (Dolag et al., in preparation). The simulation has been carried out with P-GADGET3, a modification of P-GADGET-2 (Springel 2005). The code uses an entropy-conserving formulation of SPH (Springel & Hernquist 2002) and includes treatment of radiative cooling, heating by a UV background, star formation and feedback processes from supernovae explosions and active galactic nuclei (Springel & Hernquist 2003; Fabjan et al. 2010). Cosmological parameters are chosen to match WMAP7 (Komatsu et al. 2011). The simulation box is 1244 Mpc per side and contains  $1526^3$  dark matter particles and as many gas particles, from which five simulated SZE light-cones, each of size  $13^\circ \times 13^\circ$  (i.e., the total solid angle is  $845 \text{ deg}^2$ ) have been extracted up to  $z \sim 2$ . From each of these simulated SZE maps, we then construct simulated SPT maps at 95 and 150 GHz.

The details of the construction of the simulated SZE light-cones will be presented in a forthcoming paper (Liu et al., in preparation), we highlight here the basic properties. In these mock observations, we include contributions from: (1) primary CMB anisotropies, (2) convolution with the SPT 150 GHz and 95 GHz beams, (3) instrumental noise consistent with the observed SPT map depths of 18 and  $44 \mu\text{K}$ -arcmin for the 150 GHz and 95 GHz bands, respectively, and (4) associated filter transfer functions for

the two simulated bands. Finally, from these mock maps we identify clusters with the same approach adopted for real SPT clusters (e.g., Staniszewski et al. 2009; Reichardt et al. 2013), obtaining a sample of 212 clusters above signal to noise  $\xi = 4.5$ .

We then measure the ratio of the temperatures in the two bands, using the approach described in Section 2. We first convolve the 150 GHz maps to match the larger beam of the 95 GHz band. We then individually filter the 95 GHz and the 150 GHz maps with the 95 GHz filter and measure the signal at the position and  $\theta_C$  scale that maximize the signal to noise in the multifrequency analysis. We then maximize the likelihood to determine  $\alpha$  (Eq. 3). We recover  $\alpha = 0.0019 \pm 0.022$ , in agreement with the input value of  $\alpha = 0$ .

#### 4 SPT RESULTS

We measure the temperature decrement ratios at the positions of the SPT-selected cluster sample from (Reichardt et al. 2013), which included data from 720 of the 2500 deg<sup>2</sup> SPT-SZ survey. The SPT-SZ data used here has typical noise levels of 44  $\mu\text{K}$ -arcmin and 18  $\mu\text{K}$ -arcmin in CMB temperature units at 95 GHz and 150 GHz, respectively. The exceptions are the two fields centered at  $23^h30^m, -55^d$  and  $5^h30^m, -55^d$  from Reichardt et al. (2013), which have a depth of 13  $\mu\text{K}$ -arcmin in the 150 GHz data used in this work. Since the publication of Reichardt et al. (2013), these fields had been re-observed in the SPT-SZ survey, with the new observations providing new 95 GHz measurements and deeper 150 GHz data. The final cluster sample used here consists of 158 clusters with both a  $\xi > 4.5$  from Reichardt et al. (2013), and either a spectroscopic or photometric redshift reported in Song et al. (2012). We refer the reader to Staniszewski et al. (2009), Vanderlinde et al. (2010), Schaffer et al. (2011), Williamson et al. (2011), Reichardt et al. (2013) for a detailed description of the survey strategy and dataset characteristics.

We apply the same technique described in Section 2 and tested in Section 3 to measure the evolution of the CMB temperature with SPT clusters.

Using SPT data alone, we constrain the temperature evolution of the CMB to be

$$\alpha = 0.017^{+0.030}_{-0.028}, \quad (5)$$

which is consistent with the adiabatic expectation of  $\alpha = 0$ . We estimate the instrumental uncertainties associated with the beams, calibration, and filter responses, and find them all to have a negligible result on this constraint. Moreover, the statistical uncertainty is  $\sim 30\%$  larger than the limit on possible observational biases implied by the results of Section 3, implying that our analysis method is shown to be unbiased at or below the level of the statistical uncertainty.

We further combine our results with previously published data (Fig 1). In particular we include measurements from clusters collected by Luzzi et al. (2009) and fine structure absorption line studies collected by Noterdaeme et al. (2011) and Muller et al. (2013). We thus obtain a tighter constraint on the  $T(z) = T_0(1+z)^{(1-\alpha)}$  law:

$$\alpha = 0.011 \pm 0.016, \quad (6)$$

a  $\sim 20\%$  improvement in measurement uncertainty in comparison to the previously reported  $\alpha = 0.009 \pm 0.019$  (Muller et al. 2013). We also note that previous results based on SZE measurements (Luzzi et al. 2009) have a negligible impact in this constraint.

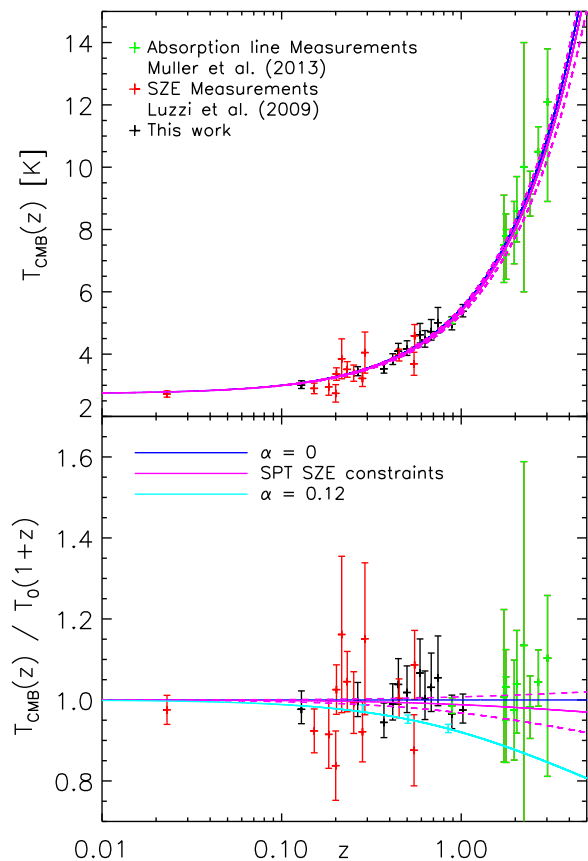


**Figure 1.** *Top panel:* Measurements of the temperature of the CMB as a function of redshift. Red points correspond to SZE measurements toward galaxy clusters (see Luzzi et al. 2009 and references therein), green points are absorption lines studies (see Muller et al. 2013 and references therein). Black points are the SPT SZE cluster constraints. For visualization purposes SPT clusters results have been stacked in 12 equally populated redshift bins. The blue continuous line corresponds to the relation  $T(z) = T_0 \times (1+z)$  and solid and dashed purple lines are the evolution corresponding to the best fit and  $\pm 1\sigma$  models. *Bottom panel:* Deviation of the measured temperature of the CMB as a function of redshift with respect to the adiabatic evolution. Cyan points represent the measured temperature of the CMB in three stacked redshift bins for a simulation with input value  $\alpha = 0.12$  (cyan solid line).

The measurement presented here is consistent with the adiabatic evolution of the CMB radiation temperature ( $\alpha = 0$ ) expected from the standard hot Big-Bang model. Considering alternative cosmological models, Jetzer et al. (2011) demonstrated that measuring  $T(z)$  at different redshifts allows one to constrain the effective equation of state of decaying dark energy ( $p = w_{\text{eff}}\rho$ ). Following Noterdaeme et al. (2011), by fitting the combined constraints on  $T(z)$  with the temperature-redshift relation (Eq. 22 in Jetzer et al. 2011), taking  $\Omega_m = 0.255 \pm 0.016$  (Reichardt et al. 2013) and fixing the adiabatic index  $\gamma$  to the canonical value (4/3), we get  $w_{\text{eff}} = -0.987^{+0.016}_{-0.017}$ , in comparison with  $w_{\text{eff}} = -0.996 \pm 0.025$  obtained by Noterdaeme et al. (2011).

#### 4.1 Selection bias

A number of possible selection biases could affect our measurements. In particular, cluster candidates were identified using a multi-band matched-filter approach (Melin et al. 2006) where the temperature evolution of the Universe is assumed to be adiabatic. This could therefore bias our selection towards clusters that best mimic this behavior. To show that this is not the case, we construct SPT mock lightcones similar to the ones presented in Sect. 3 but assuming different values of  $\alpha$ . We then performed the same analysis described in Sect. 3 and show that we are able to recover the input value. Specifically we test simulations with input values of  $\alpha$  offset by more than  $3\sigma$  from the adiabatic value,  $\alpha = -0.12$  and  $\alpha = 0.12$ . We then select clusters with the above described matched-filter multi-frequency cluster finder under the assumption of adiabatic evolution and constrain  $\alpha$ . We obtain unbiased measurements for the underlying input value  $\alpha = -0.111_{-0.018}^{+0.022}$  and  $\alpha = 0.110_{-0.014}^{+0.014}$ , thus demonstrating that the selection is not driving our constraints (bottom panel of Fig. 1).

Another potential source of bias in our measurement of  $\alpha$  is the fact that the temperature fluctuations of the CMB at the location of the SPT clusters should not average to zero. In fact, due to the adopted cluster selection, negative temperature fluctuations are more likely than positive ones (Vanderlinde et al. 2010). We estimate this effect to be negligible using the simulations described in Sect. 3. We also note that this effect should be less significant at larger SPT signal to noise  $\xi$  (Benson et al. 2013). If we restrict our analysis to the clusters with  $\xi > 8$ , which reduces the cluster sample by a factor of  $\sim 6$  to the 24 highest signal-to-noise clusters, we constrain  $\alpha = 0.023_{-0.038}^{+0.044}$ . This is consistent with our main result with only a modest 30% increase in the uncertainty in  $\alpha$ . This demonstrates that the constraints depend most significantly on the highest signal to noise clusters, which will be less biased by the CMB from the SPT-selection. Similarly, we estimate the bias associated with lensed dusty sources to be unimportant for our analysis; their primary impact would be introducing some skewness in the scatter of clusters about our best fit model (Hezaveh et al. 2013).

Emission from cluster galaxies can also potentially bias our measurement. We estimate the effect to be negligible by performing the analysis presented here on subsamples of clusters above different  $\xi$  thresholds and by excluding clusters in proximity to known SUMSS sources (Mauch et al. 2003). All subsamples examined provide statistically consistent results. For example, using a subsample of 75 clusters with no associated SUMSS sources brighter than 20 mJy within a projected distance of 3 arcmin from the cluster centers, we obtain consistent results of  $\alpha = 0.021_{-0.038}^{+0.042}$ .

## 5 CONCLUSIONS

We have studied deviations from the adiabatic evolution of the mean temperature of the CMB in the form of  $T(z) = T_0(1+z)^{(1-\alpha)}$ . We present a method based on matched-filtering of clusters at the SPT frequencies and show that we are able to recover unbiased results using simulated clusters. The simulated lightcones we use come from a large cosmological hydrodynamical simulation and include realistic SPT beam effects, CMB anisotropy and SPT noise levels for both the 150 GHz and 95 GHz bands.

We apply this method to a sample of 158 SPT clusters selected from 720 square degrees of the 2500 square degree SPT-SZ survey, which span the redshift range  $0.05 < z < 1.35$ , and measure  $\alpha = 0.017_{-0.028}^{+0.030}$ , consistent with the standard model pre-

diction of  $\alpha = 0$ . Our measurement gives competitive constraints and significantly extends the redshift range with respect to previously published results based on galaxy clusters (e.g., Luzzi et al. 2009; Avgoustidis et al. 2012; de Martino et al. 2012; Muller et al. 2013). Combining our measurements with published data we obtain  $\alpha = 0.011 \pm 0.016$ , a 20% improvement with respect to current published constraints.

Such tight limits on deviations from the adiabatic evolution of the CMB also put interesting constraints on the effective equation of state of decaying dark energy models,  $w_{\text{eff}}$ . Indeed, from SPT clusters alone we are able to measure  $w_{\text{eff}} = -0.988_{-0.033}^{+0.029}$ , in good agreement with previous constraints based on quasar absorption lines (Noterdaeme et al. 2011).

Coincident with the submission of this analysis, Hurier et al. (2013) released results of a similar analysis carried out on 1839 galaxy clusters observed with Planck. The cluster sample they adopted also included the SPT sample that we analyse here, although it did not contribute significantly to their main results. They were able to constrain  $\alpha = 0.009 \pm 0.017$  by stacking the Planck catalog of SZE detected clusters (Planck Collaboration 2013) in different redshift bins, with only one cluster in each of their highest redshift bins  $z = 0.8$  and  $z = 1$ . Because the SPT data are on average a factor of 3 deeper than Planck, and the SPT beam is  $\sim 8$  times smaller, the SPT dataset provides stronger constraints on a per cluster basis and is particularly well suited for studies of the high redshift tail of the cluster distribution.

Future analyses will be able to draw upon larger cluster samples (e.g., the full 2500 square degree SPT-SZ survey and the upcoming SPTpol and SPT-3G surveys) and quasar surveys (e.g., SDSS III). By expanding the data volume at high redshifts, these surveys will enable precision tests of the temperature evolution of the CMB across cosmic time. Moreover, because clusters and quasars suffer from different systematics, the comparison will provide an important cross-check on systematics. These surveys will improve constraints on non-standard cosmological models.

The Munich SPT group is supported by the DFG through TR33 ‘‘The Dark Universe’’ and the Cluster of Excellence ‘‘Origin and Structure of the Universe’’. The South Pole Telescope program is supported by the National Science Foundation through grant ANT-0638937. Partial support is also provided by the NSF Physics Frontier Center grant PHY-0114422 to the Kavli Institute of Cosmological Physics at the University of Chicago, by the Kavli Foundation and the Gordon and Betty Moore Foundation. Galaxy cluster research at Harvard is supported by NSF grants AST-1009012 and DGE-1144152. Galaxy cluster research at SAO is supported in part by NSF grants AST-1009649 and MRI-0723073. The McGill group acknowledges funding from the National Sciences and Engineering Research Council of Canada, Canada Research Chairs program, and the Canadian Institute for Advanced Research.

## REFERENCES

- Avgoustidis A., Luzzi G., Martins C. J. A. P., Monteiro A. M. R. V. L., 2012, *J. Chem. Phys.*, 2, 13
- Battistelli E. S. et al., 2002, *ApJ*, 580, L101
- Benson B. A. et al., 2013, *ApJ*, 763, 147
- Carlstrom J. E. et al., 2011, *PASP*, 123, 568
- Cavaliere A., Fusco-Femiano R., 1976, *A&A*, 49, 137
- de Martino I., Atrio-Barandela F., da Silva A., Ebeling H., Kashlinsky A., Kocevski D., Martins C. J. A. P., 2012, *ApJ*, 757, 144
- Fabrizi R., Melchiorri F., Natale V., 1978, *Ap&SS*, 59, 223

- Fabjan D., Borgani S., Tornatore L., Saro A., Murante G., Dolag K., 2010, MNRAS, 401, 1670
- Fixsen D. J. et al., 2009, submitted to ApJ, astro-ph/0901.0555
- Hezaveh Y., Vanderlinde K., Holder G., de Haan T., 2013, ApJ, 772, 121
- Hurier G., Aghanim N., Douspis M., Pointecouteau E., 2013, ArXiv e-prints:1311.4694
- Itoh N., Kohyama Y., Nozawa S., 1998, ApJ, 502, 7
- Jaeckel J., Ringwald A., 2010, Annual Review of Nuclear and Particle Science, 60, 405
- Jetzer P., Puy D., Signore M., Tortora C., 2011, General Relativity and Gravitation, 43, 1083
- Jetzer P., Tortora C., 2011, Phys. Rev. D, 84, 043517
- Komatsu E. et al., 2011, ApJS, 192, 18
- Lima J. A. S., Silva A. I., Viegas S. M., 2000, MNRAS, 312, 747
- Luzzi G., Shimon M., Lamagna L., Rephaeli Y., De Petris M., Conte A., De Gregori S., Battistelli E. S., 2009, ApJ, 705, 1122
- Martins C. J. A. P., 2002, Royal Society of London Philosophical Transactions Series A, 360, 2681
- Matyjasek J., 1995, Phys. Rev. D, 51, 4154
- Mauch T., Murphy T., Buttery H. J., Curran J., Hunstead R. W., Piestrzynski B., Robertson J. G., Sadler E. M., 2003, MNRAS, 342, 1117
- Melin J.-B., Bartlett J. G., Delabrouille J., 2006, A&A, 459, 341
- Molaro P., Levshakov S. A., Dessauges-Zavadsky M., D'Odorico S., 2002, A&A, 381, L64
- Muller S. et al., 2013, A&A, 551, A109
- Murphy M. T., Webb J. K., Flambaum V. V., 2003, MNRAS, 345, 609
- Noterdaeme P., Petitjean P., Srianand R., Ledoux C., López S., 2011, A&A, 526, L7
- Overduin J. M., Cooperstock F. I., 1998, Phys. Rev. D, 58, 043506
- Planck Collaboration, 2013, ArXiv e-prints:1303.5089
- Puy D., 2004, A&A, 422, 1
- Reichardt C. L. et al., 2013, ApJ, 763, 127
- Rephaeli Y., 1980, ApJ, 241, 858
- Schaffer K. K. et al., 2011, ApJ, 743, 90
- Song J. et al., 2012, ApJ, 761, 22
- Springel V., Hernquist L., 2003, MNRAS, 339, 289
- Srianand R., Chand H., Petitjean P., Aracil B., 2004, Physical Review Letters, 92, 121302
- Srianand R., Noterdaeme P., Ledoux C., Petitjean P., 2008, A&A, 482, L39
- Srianand R., Petitjean P., Ledoux C., 2000, Nature, 408, 931
- Staniszewski Z. et al., 2009, ApJ, 701, 32
- Sunyaev R. A., Zel'dovich Y. B., 1972, Comments on Astrophysics and Space Physics, 4, 173
- Vanderlinde K. et al., 2010, ApJ, 722, 1180
- Williamson R. et al., 2011, ApJ, 738, 139